TOPICAL REVIEW — Statistical physics and complex systems

Attractive target wave patterns in complex networks consisting of excitable nodes*

Zhang Li-Sheng(张立升)[a], Liao Xu-Hong(廖旭红)[b], Mi Yuan-Yuan(弭元元)[a,c], Qian Yu(钱 郁)[d], and Hu Gang(胡 岗)[e,†]

[a] State Key Laboratory of Cognitive Neuroscience and Learning, International Digital Group (IDG)/McGovern Institute for Brain Research, and Center for Collaboration and Innovation in Brain and Learning Sciences, Beijing Normal University, Beijing 100875, China
[b] Center for Cognition and Brain Disorders, Hangzhou Normal University, Hangzhou 310036, China
[c] Center for Systems Biology, Soochow University, Suzhou 215006, China
[d] School of Physics and Information Technology, Baoji University of Arts and Sciences, Baoji 721013, China
[e] Department of Physics, Beijing Normal University, Beijing 100875, China

(Received 17 June 2014; published online 24 June 2014)

This review describes the investigations of oscillatory complex networks consisting of excitable nodes, focusing on the target wave patterns or say the target wave attractors. A method of dominant phase advanced driving (DPAD) is introduced to reveal the dynamic structures in the networks supporting oscillations, such as the oscillation sources and the main excitation propagation paths from the sources to the whole networks. The target center nodes and their drivers are regarded as the key nodes which can completely determine the corresponding target wave patterns. Therefore, the center (say node A) and its driver (say node B) of a target wave can be used as a label, (A,B), of the given target pattern. The label can give a clue to conveniently retrieve, suppress, and control the target waves. Statistical investigations, both theoretically from the label analysis and numerically from direct simulations of network dynamics, show that there exist huge numbers of target wave attractors in excitable complex networks if the system size is large, and all these attractors can be labeled and easily controlled based on the information given by the labels. The possible applications of the physical ideas and the mathematical methods about multiplicity and labelability of attractors to memory problems of neural networks are briefly discussed.

Keywords: dominant phase advanced driving method, complex networks, labelable attractors, target wave patterns

PACS: 89.75.Fb, 89.75.Kd, 05.65.+b **DOI:** 10.1088/1674-1056/23/7/078906

1. Introduction

Pattern formation and pattern dynamics have been one of the central issues in statistical physics, thermodynamics, and nonlinear science for more than a century.[1,2] For a long period, they have been studied in regular media.[3–6] In the recent two decades, complex networks have attracted great interest,[7–9] and thus pattern dynamics in complex networks has become an extremely hot topic in both natural and social sciences.[10–12]

Self-sustained oscillatory patterns are one of the important patterns in nature, in particularly, oscillations in complex networks consisting of non-oscillatory units,[13,14] such as gene regulatory networks,[15] neural networks,[16] and epidemic spreads,[11,17] play important roles in determining various functional rhythmics. In many practical systems, networks generating oscillations are complicated and the output data may be huge. The underlying organizations of the oscillations may be deeply hidden in the complex networks and the output data. Therefore, some intelligent physical and mathematical methods comprehensively analyzing the available data for understanding the simple structures existing in the oscillations of complicated networks become crucial from both theoretical and practical points of view.[13,18–20]

In this article, we review some recent works of our group in this direction.[13,14,21,22] We take oscillatory networks consisting of excitable nodes as examples. The relevance of this type of networks to the practical neural networks is emphasized since excitability of network nodes and complexity of network structures are two major characteristic features of neural networks. This article is organized as follows. In Section 2, we specify the model and propose a method called the dominant phase advanced driving (DPAD) method to analyze oscillatory excitable networks. In Section 3, the DPAD method is applied to the excitable network model to reveal and analyze target wave patterns, where target centers, oscillation source loops, and wave propagation paths in the networks are understood clearly based on the DPAD analysis. In Section 4, we go further to study multiple attractors of oscillating ex-

*Project supported by the National Natural Science Foundation of China (Grant Nos. 11174034, 11135001, 11205041, and 11305112) and the Natural Science Foundation of Jiangsu Province, China (Grant No. BK20130282).

†Corresponding author. E-mail: ganghu@bnu.edu.cn

© 2014 Chinese Physical Society and IOP Publishing Ltd

citable networks, including multiplicity of attractors, labellability of multiple targets, and effective generation and control of attractors based on their labels. In Section 5, statistical investigation on target wave patterns is carried out, labelable attractors are computed based on both theoretical label analysis and numerical computation of network dynamics. Coexistence and predictability of huge number of target wave attractors are confirmed. The last section provides brief discussion and conclusion.

2. Model and DPAD method

We consider networks of N Bär nodes

$$\begin{aligned}\frac{\mathrm{d}u_i}{\mathrm{d}t} &= -\frac{1}{\varepsilon}u_i(u_i-1)\left(u_i-\frac{v_i+b}{a}\right)\\ &\quad +D_u\left(\frac{\sum_{j=1}^{N}M_{ij}u_j}{\sum_{j=1}^{N}M_{ij}u_j+K}-u_i\right),\\ \frac{\mathrm{d}v_i}{\mathrm{d}t} &= f(u_i-v_i),\quad i=1,2,\ldots,N,\end{aligned}\tag{1}$$

where $f(u_i)=0, f(u_i)=1-6.75u_i(u_i-1)^2$, and $f(u_i)=1$ for $u_i\le 1/3$, $1/3\le u_i\le 1$, and $u_i\ge 1$, respectively. Here the parameters used ($a=0.84$, $b=0.07$, $\varepsilon=0.04$) can guarantee the excitable local dynamics.[23] The coupling matrix is defined as $M_{ij}=1$ if i and j are connected and $M_{ij}=0$ otherwise. The symmetric couplings with $D_u=0.4$ and $K=0.8$ make sure that each excitation of any node can promote successful excitations of the neighbor nodes at rest state. The topological structures of the networks may be diverse, such as Erdös–Rényi,[9,24,25] small-world,[7] and scale-free[8] structures. For simplicity, we focus on homogeneous random networks (HRNs),[18,19] where the connection degree of each node is identical.

An obvious characteristic feature of Eq. (1) is that all nodes in the network cannot oscillate individually, a node can sustainedly oscillate only when it is driven by other nodes. This principle is hold by all nodes. In self-sustainedly oscillatory networks, any network with all nodes driven by the other nodes must have the following universal structure: (i) there must be some (at least one) loops with nodes driven successively; and (ii) all off-loop nodes must be in various chains of successively driving nodes rooted from one or more of the loop nodes. The structure is schematically shown in Fig. 1(a). The universality of these driving relations is for the class of sustainedly oscillatory networks consisting of non-oscillatory nodes. And the excitable complex networks (ECNs) are certainly of this type.

From the above analysis, loop structures are important for network oscillations. According to the graph theory, for any connected network with N nodes and M ($M\ge N$) interactions, the number of fundamental cycles (fundamental cycles are loops that contain at least one node which all other loops do not have) is $M-N+1$.[26] And the number of topologically different cycle sets serving as the candidates of source is 2^{M-N+1}, which is huge in the case of $M-N\gg 1$ (this happens for most practical complex networks). Therefore, finding some key loops generating network oscillations from the huge number of candidate loops is a crucial and seemly difficult task in the analysis of network oscillations.

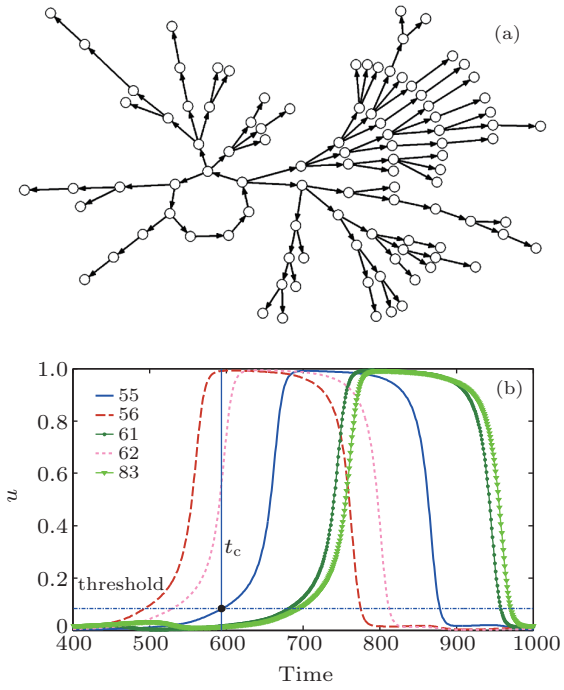


Fig. 1. (a) Schematic illustration of periodically oscillatory 1D networks consisting of nonoscillatory nodes. This type of networks display a universal form of tree branches radiating from an interacting loop, satisfying a principle that all nodes must be driven by other nodes to oscillation. (b) Demonstration of the phase advanced driving and the dominant phase advanced driving of a given node 55. Nodes 56 and 62 are the phase advanced driving of node 55. And node 56 is the dominant phase advanced driving.

For different systems, there are different ways for defining the relationships between nodes. Generally, for a given node, we define the interactions from its neighbors as phase advanced (phase delay) drivings which are favorable to drive the given node to oscillation (draw back the given node from oscillation). Among all phase advanced drivings, there is one making the most important contribution, called the dominant phase advanced driving (DPAD). In Fig. 1(b), we show how to identify phase advanced driving and DPAD in an actual oscillatory excitable network. For a given node i (node 55 in Fig. 1(b)), we define phase advanced drivings as the interactions from all its neighbor j's (nodes 56 and 62) which have $u_j(t)>u_i(t)$ at time t_c when the given node i is kicked from the rest state, crossing the threshold $u_c=b/a$, to excitation. Among all these phase advanced drivings, we further define the driving from the node which has the largest $u(t)$ at t_c (node 56) as the DPAD.

Now the DPAD method can be summarized as follows. (i) By studying the data of network oscillation, find phase advanced driving interactions for each node. (ii) Find the single DPAD for each given node among its phase advanced drivings. (iii) Use all these DPADs to directedly link all the network nodes and draw the DPAD subnetwork (or say the DPAD pattern).

The DPAD subnetworks can be incomparably simpler than the original topological networks. In a connected network of N nodes and M interactions, there are 2^{M-N+1} loops serving as the possible oscillation sources. However, its DPAD subnetwork has N nodes and N links (each node has one and only one DPAD). Thus, the DPAD subnetworks are one-dimensional (1D) networks, and each connected DPAD network has one and only one loop ($2^{M-N+1}-1=1$), which is just the oscillation source, and all the DPAD chains rooted from the loop demonstrate the paths of signal propagations in the oscillatory network.

3. Target waves in excitable networks

Figure 2 shows some examples of oscillatory patterns of a homogeneous ECN. The network structure is displayed in Fig. 2(a). For random initial conditions, the network has more than 95% probability to approach periodic oscillations, 961 different oscillations are observed with 10^3 tests. In Fig. 2(b), average signals $\langle u(t)\rangle = \frac{1}{N}\sum_{i=1}^{N} u_i(t)$ are plotted for three different patterns, and the corresponding snapshots of the patterns are plotted in Figs. 2(c) (oscillation A), 2(d) (oscillation B), and 2(e) (oscillation C), respectively. Different colors in Figs. 2(c)–2(e) represent different phases of oscillations. All these snapshots look rather random, one can hardly see any traces of the structures of the given patterns. We need to disturb the system and study the system response.

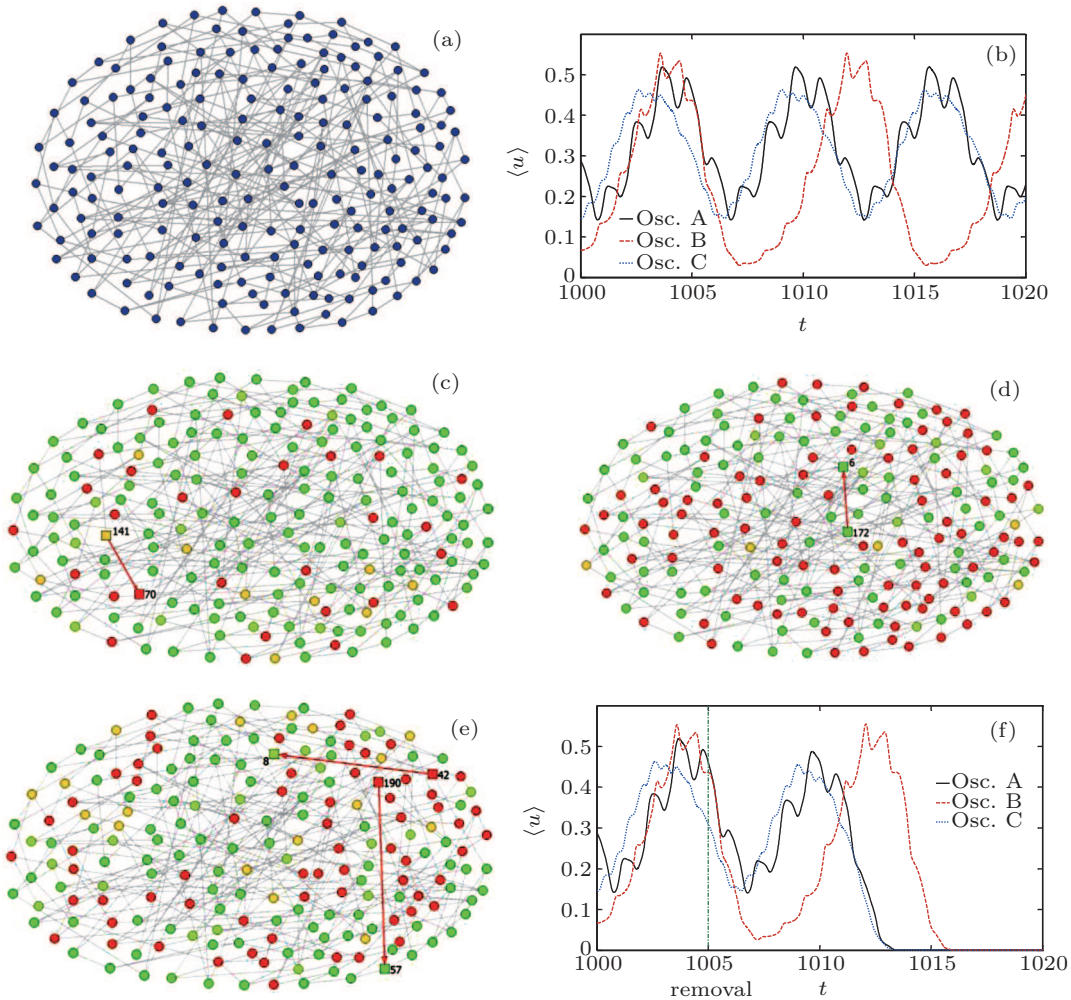


Fig. 2. (a) Homogeneous random network studied ($N=200$, $k=3$). The network dynamics is described by Eq. (1) with parameters $a=0.84$, $b=0.07$, $\varepsilon=0.04$, $D_u=0.4$, and $K=0.8$. All these parameters are used in Figs. 1–6. (b) Periodic time evolution of $\langle u(t)\rangle = \frac{1}{N}\sum_{i=1}^{N} u_i(t)$ for three different random initial conditions. These three oscillations are denoted as oscillations A, B, and C, respectively. (c) Snapshot of oscillation A at a certain time. The phase distribution (i.e., the distribution of different colors) among different nodes seems random. In the following figures, all snapshots are displayed with local variable u plotted without further remarks, and the arrowed links in all figures represent the dynamical driving relationship. (d) and (e) Snapshots of oscillations B and C, respectively. (f) Suppression of oscillations A, B, and C by removing square nodes 70, 6, and (8, 57) at $t=1005$, respectively. The time of the node removal is denoted by the vertical dashed line ($t=1005$).[13]

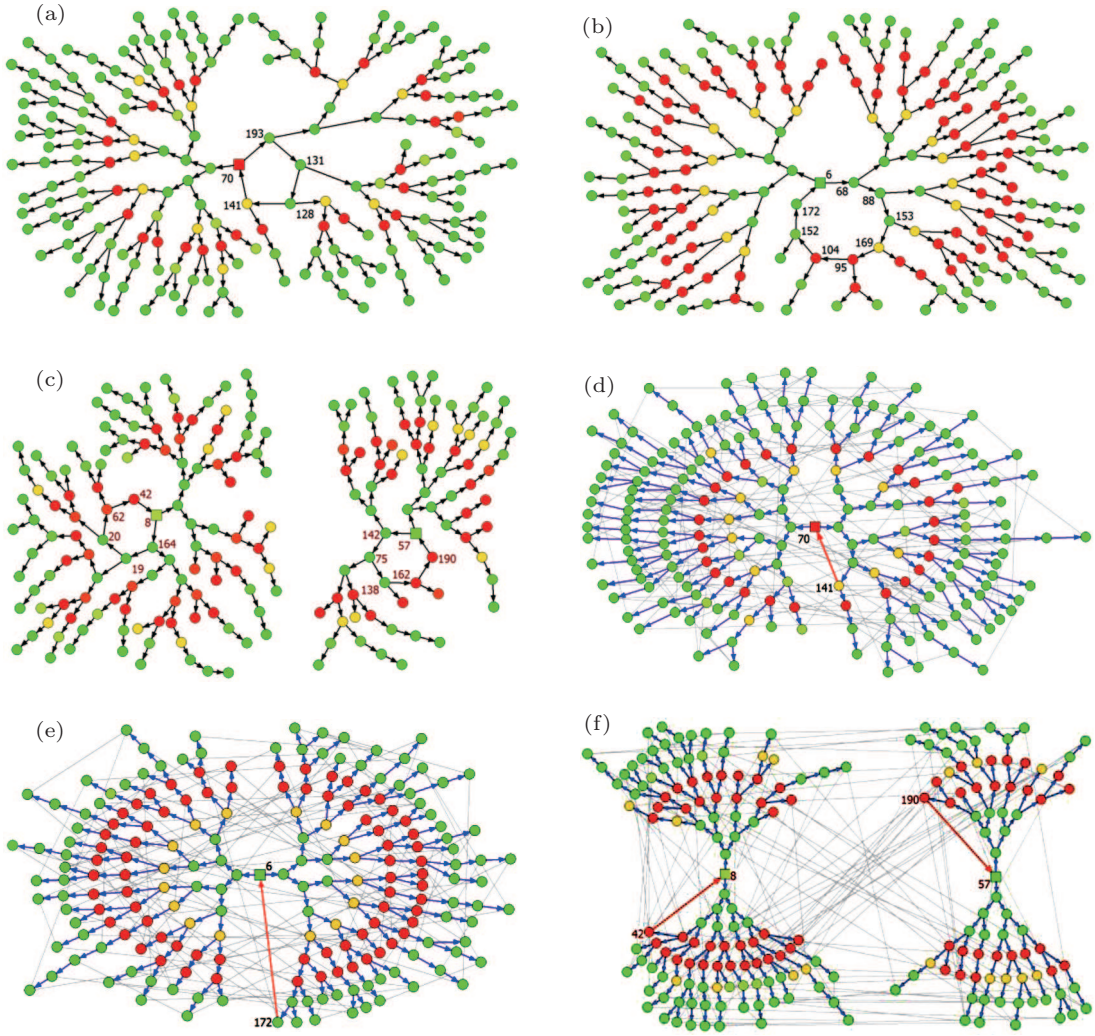


Fig. 3. (a)–(c) DPAD patterns of the oscillatory states A, B, C in Figs. 2(c)–2(e), respectively. In panles (a) and (b), single source loops are observed, while in panel (c), we identify two clusters of nodes dominated by two source loops separately. (d) Snapshot the same as that in Fig. 2(c) for oscillation A, with each node placed around center node 70 according to the distance from the center. The purple (dark) lines show the shortest paths from center node 70 to the other nodes, while the gray (light) lines indicate all the other interactions between different nodes. Perfect target waves propagating from center node 70 are observed. The bold arrow denotes the driving from driving node 141 to center node 70. (e) Snapshot the same as that in Fig. 2(d) for oscillation B. The target center is node 6, while its driver is node 172. (f) Snapshot the same as that in Fig. 2(e) for oscillation C, with nodes placed around two centers 8 and 57. A 2-center target pattern is identified.[13]

For the states in Figs. 2(c)–2(e), we remove some nodes and investigate the network evolutions after the removals. In most cases, oscillations A, B, and C are robust against the removals of few nodes. However, these oscillations are sensitive to the removals of some specific nodes called key nodes. All these key nodes are marked in Figs. 2(c)–2(e) by squares. Both oscillations A and B can be suppressed by just removing a single node (one of (70, 141) pair for A and one of (6, 172) pair for B). While for oscillation C, the oscillation can never be terminated by discarding any single node, instead one has to remove two nodes simultaneously for suppressing the oscillation, one from pair $(8,42)$ and the other from pair $(57,190)$. In Fig. 2(f), we plot $\langle u(t)\rangle$ as in Fig. 2(b) with some key nodes discarded at a certain moment ($t = 1005$), where oscillation terminations are clearly shown after the key nodes are controlled. The diverse behaviors shown in Fig. 2 indicate that though the network structure and the parameter distribution are homogeneous, different nodes play significantly different roles. To reveal these different roles of the nodes and thus to understand the related dynamical structures are the central tasks in this section.

Now we apply the DPAD method to the three patterns in Fig. 2 by analyzing the output data of the states. The three DPAD patterns are given in Figs. 3(a)–3(c). Some interesting features in the figures are worthwhile remarking. First, the universal structure predicted in Fig. 1(a) is indeed observed in all these DPAD subnetworks. In all figures, there are one (Figs. 3(a) and 3(b)) or a few (two in Fig. 3(c)) loops in the DPAD patterns serving as the oscillation sources of the networks, and all off-loop nodes are in chains or branches of chains rooted from the loop nodes acting as the main signal propagation paths. Second, all key nodes (squares) in Fig. 2

are located on the source loops of the DPAD patterns. Discarding a key node in Fig. 3(a) (also in Fig. 3(b)) can destroy the source loop and thus suppress the network oscillation. On the other hand, in Fig. 3(c), there are two source loops in the DPAD network. Breaking a single loop cannot completely destroy the oscillation source (the remaining survived loop can still play the role of oscillation source). This is why one needs to discard two key nodes from different loops simultaneously to destroy both existing DPAD source loops. All these observations in the DPAD patterns fully agree with the depicted features of the key nodes.

However, there still exists one feature in Fig. 3 that cannot be directly explained by the DPAD loop analysis. There are many nodes in the source loops in Figs. 3(a)–3(c) among which only a few key nodes shown in Figs. 2(c)–2(e) are sensitive for the oscillation suppression. By deeply studying the relationships between the key nodes, we can find that each pair of two nodes are connected and in the DPAD patterns, one of a pair of nodes is driven by its partner (i.e., $140 \rightarrow 70$ in Fig. 3(a), $172 \rightarrow 6$ in Fig. 3(b), and $42 \rightarrow 8, 190 \rightarrow 57$ in Fig. 3(c)). We thus call the key nodes driven by their partners as the driven key nodes (i.e., nodes 70, 6, 8, 57 in Fig. 3) while their partners as the driving key nodes (key nodes 141, 172, 42, 190 in Fig. 3). All driven key nodes have a large number of downstream branches of nodes, while the driving key nodes have very small number of downstream nodes or even have no branching node. We assume that the driven key nodes are the center nodes for the given oscillations while the driving nodes serve as the drivers of the centers.

In Figs. 3(d)–3(f), we draw exactly the same patterns as those in Figs. 3(a)–3(c), with slight reformation by placing all centers at the central parts and all other nodes layer by layer according to their shortest distances from the centers. Here all arrowed links represent DPADs. The colors of all nodes in Figs. 3(d)–3(f) are identical with those in the snapshots of Figs. 2(c)–2(e). It is surprising that the randomly distributed color nodes in Fig. 2 are replaced with completely regular target wave organizations. In Figs. 3(d)–3(f), three main features are observed. (i) Waves propagate from the center nodes to the whole networks along the shortest paths. (ii) The shortest loop, which passes through both the centers and their drivers, plays the role of the oscillation source and determines the oscillation features (e.g., the oscillation frequency). (iii) The centers are driven by their drivers for sustaining their oscillations, and the latter are driven in turn by the former through the wave propagation in the source loops. With the target waves in Figs. 3(d)–3(f), we can well understand why the key nodes are so much different from the other nodes in the source loops. The target centers are the origins for the target wave propagations. Discarding the center of a target wave pattern can surely terminate the given target pattern. On the other hand, the sustained oscillation of the target center is maintained by its driver, and thus removing the driver can also suppress the given target wave. If we remove a node in a source loop other than the center and the driver, the original source loop is certainly broken. However, the oscillation wave starting from the center can often find a new path to reach the driver through other interactions which are not DPADs before the loop node removal while become DPADs after the removal. Then the functions of the center and the driver are not affected though the source loop does have been changed, and the oscillation survives.

4. Complex excitable networks with large numbers of labelable attractors

Neural systems have extremely rich fascinating functions, among which the memory is the most mystery one. The brain can keep a large amount of information, easily retrieve a wanted memory from the rich reservoir of memories on purpose, and also easily stop a memory representation and change from one memory to another. The brain works as a complex network consisting of a huge number of neurons possessing excitable dynamics.[27] And it is accepted to a certain extent that memories can be understood as attractors in the neural networks of the brain.[28,29] In the following part of this paper, we will not consider how the brain can biologically create, keep, and retrieve memories. Instead, we investigate much simpler dynamic problems: how can ECNs allow an extremely large number of attractors, how can one easily enter a wanted attractor among so many attractors, and how can one readily manipulate presentation among different attractors. These tasks are nontrivial since in case of many attractors, each attractor has only a very small basin of attraction and the boundaries between different basins are very complicated (e.g., the boundaries often have fractal nature).

In Section 3, we showed that ECNs can display many different oscillatory patterns (i.e., oscillatory attractors). Here we focus on the analysis of this type of attractors. We start from a network of Eq. (1) with nodes coupled in a 1D ring structure as shown in Fig. 4(a). A simple way to generate a sustainedly oscillatory attractor in a loop from the all-rest state is to excite any node in the loop (say node A) and simultaneously block the excitation propagation to one of its neighbors (say neighbor B). We call this type of excitation as (A,B) excitation (see Fig. 4(a)). The (A,B) excitation can break the symmetry of the loop and create the directed excitation propagation denoted in Fig. 4(a). And the propagation finally excites node B and node B excites node A again, this makes the oscillation sustained. An oscillatory attractor created by the (A,B) excitation is called the (A,B) attractor with (A,B) being the label of this attractor. By varying nodes A and B, we can realize different attractors. However, for the 1D loop, there are only two

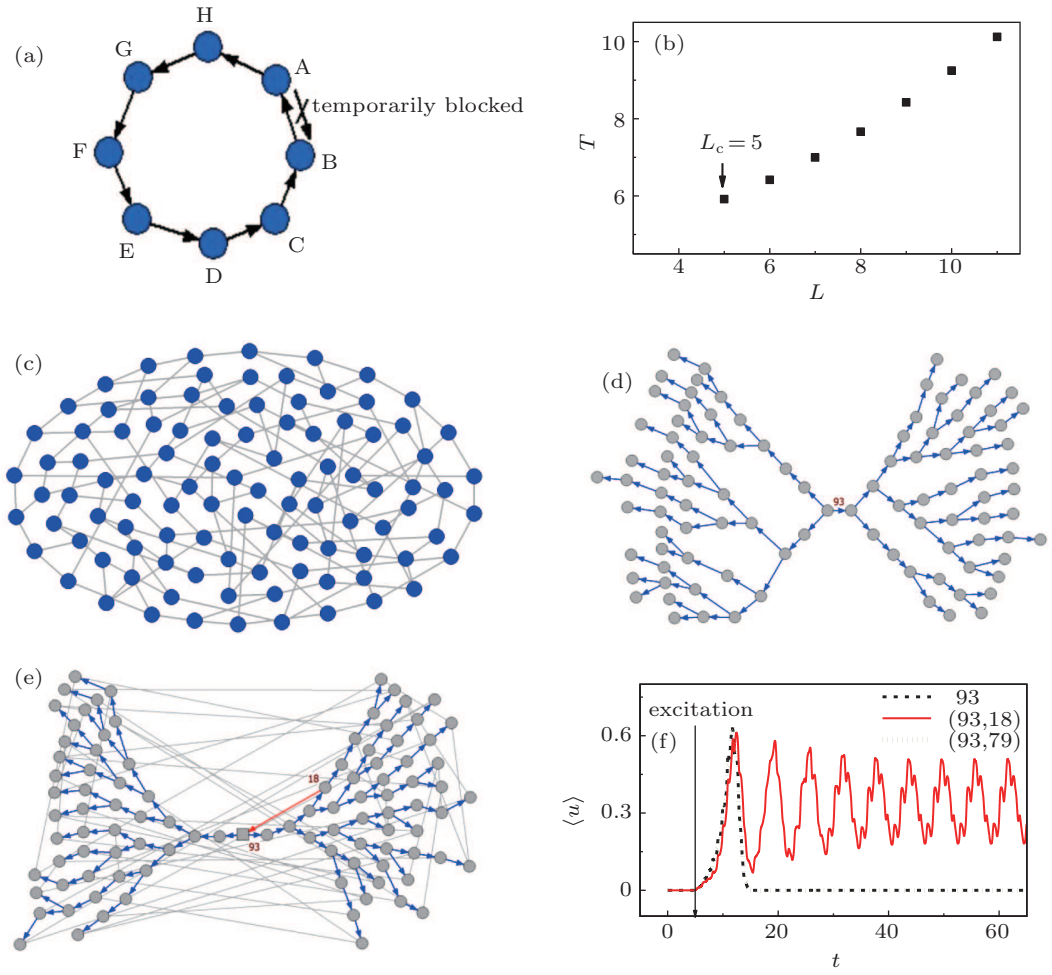


Fig. 4. The (A,B) excitation and (A,B) label of an oscillatory attractor. (a) Schematic illustration of the (A,B) excitation method in a 1D loop of symmetrically coupled excitable nodes. The (A,B) excitation is to stimulate node A with its interaction to a neighbor node B blocked during the initial excitations of node A. The arrows indicate the direction of the excitation propagation (i.e., the dynamic driving relations). (b) Period T versus loop length L for the 1D loop. There is a critical loop length $L_c = 5$ with the parameters of Eq. (1), smaller than which the 1D loop cannot support a persistent oscillation. (c) Homogeneous random network considered with $N = 100$ and $k = 3$. (d) Identical network as in panel (c) with a new arrangement by fixing an arbitrary node $A = 93$ at the center and placing all the other nodes according to their shortest distances from node 93. The purple dark arrows indicate the shortest paths and the thin gray links represent all the other interactions. An excitation of center node $A = 93$ can cause transient target waves along the arrows. The oscillation dies (shown in panel (f)) after the transient. (e) Snapshot of the oscillation generated by the $(93,18)$ excitation ($L_{\min}(93,18) = 5$). The red-arrowed loop (the shortest loop passing through nodes 93 and 18) is the oscillation source. (f) Numerical results of evolution $\langle u(t)\rangle = \sum_{i=1}^{N} u_i(t)/N$ caused by 93 $(93,18)$, and $(93,79)$ excitations.[14]

oscillatory attractors distinguished with clockwise and anti-clockwise excitation propagations. Simply shifting the (A,B) position in the loop leads to the same excitation propagation state, i.e., the same attractor. The oscillation period on the loop depends on the loop size. In Fig. 4(b), period T is plotted against loop size L, and a nearly linear dependence of T–L is observed. In Fig. 4(b), there is a minimum $L = L_c$ ($L_c = 5$ for the parameters used in Eq. (1)), if $L < L_c$, the 1D loop cannot support a self-sustained oscillation due to the existence of the refractory period of excitable dynamics.

The (A,B) excitation analysis can be applied to general ECNs. Let us consider another homogeneous ECN with $N = 100$ and $k = 3$ in Fig. 4(c). From an all-rest state, we demonstrate how to generate a sustainedly oscillatory pattern. First, we can try to directly excite the network by applying an instant pulse to an arbitrary node, say A = node 93, called the A excitation. Then the excitation can propagate from node 93 to other nodes via the shortest paths (see Fig. 4(d)). All nodes undergo excited, refractory states and finally reach the rest state. Since no mechanism reactivates any node, the network goes to the all-rest state and stay there forever. Now we apply the (A,B) excitation to the all-rest state of the ENC in Fig. 4(c) with $A = 93$ and $B = 18$. In Fig. 4(e), after node A is excited, the excitation propagates to all the nearest neighbors (nodes 62 and 79) except node 18 which is blocked as the B node. The excitation propagates layer by layer through the shortest paths similar to that in Fig. 4(d). An important difference between Figs. 4(e) and 4(d) is that node 18 in Fig. 4(e) is excited after four propagation steps (see the red arrows in Fig. 4(e)) and then reexcites node 93 via the shortest loop through (A,B). Since the minimum length passing (A,B) is $L_{\min}(A,B) = L_c = 5$, node A has recovered to the excitable

state after its refractory period when the stimulation from node B arrives. Then node B can succeed to excite node A, and the reexcited node A can repeat its excitation propagation and thus sustain the persistent oscillation in the network. The (A,B) excitation can be applied to different node pairs in the ECN. For instance, in Fig. 4(c), we can also make the (93, 79) excitation. In this case, the reexcitation from node B to node A must fail since $L_{\min}(93,79) = 3 < L_c = 5$. In Fig. 4(f), we show the time evolutions of $\langle u \rangle$ for successful (93, 18) and failed ((93) and (93, 79)) stimulations. It is emphasized that each oscillatory pattern generated by the (A,B) excitation is nothing but the target wave discussed in Section 3 and shown in Fig. 3. In the resulting (A,B) attractor, there are three significant ingredients: node A plays the role of the target center; node B serves as the driver of the center for supporting the rexcitation of node A and sustains the oscillation of the ECN; the shortest loop going through nodes A and B (the red loop in Fig. 4(e)) is the oscillation source determining various characteristic features of the network dynamics, such as the oscillation frequency. The oscillation in Fig. 4(e) can be conveniently terminated by suppressing the excitation of a single node A and thus be called a one-center target wave attractor. One can extend the single-center (A,B) excitation to two-center excitation $(A_1,B_1)(A_2,B_2)$ with A_1, A_2 being the two centers and B_1, B_2 being their corresponding drivers; and to multiple center excitation $(A_1,B_1)(A_2,B_2)(A_1,B_1)\cdots(A_M,B_M)$ with M centers $A_1,A_2,\ldots,A_M$ and their M drivers.

We now theoretically analyze the excitations with different numbers of centers. Let us firstly consider one center (A,B) oscillatory attractor which requres

$$L_{\min}(A,B) \geq L_c. \tag{2}$$

Obviously, equation (2) is necessary, otherwise node B cannot reexcite node A to sustain the oscillation. This condition is also sufficient, as whenever successful reexcitation of node A by node B is guaranteed, the oscillation of the ECN can be self-sustained. Moreover, the oscillatory pattern generated by the (A,B) excitation is an attractor because the state is stable against sufficiently small perturbations which cannot change the threshold barriers of the excitation. This attractor is labeled as (A,B). Nodes A and B can be chosen arbitrarily among the N network nodes provided condition (2) and another condition that nodes A and B are directly connected are satisfied. Thus the number of (A,B) one-center attractors can be computed as

$$M_1 = \sum_{i=1}^{N} k_i - I_1 \lesssim N\langle k \rangle, \tag{3}$$

where I_1 is the number of all (A,B) with $L_{\min}(A,B) < L_c$ and $\langle k \rangle$ is the average degree of the network. Usually, $I \ll N\langle k \rangle$ for large N and sparse networks.

For a two-center excitation $(A_1,B_1)(A_2,B_2)$, nodes A_1 and A_2 are excited together with their corresponding drivers B_1 and B_2 being temporally blocked during the initial excitation of A_1 and A_2. Nodes A_1 and A_2 should be reexcited by nodes B_1 and B_2, respectively, while nodes B_1 and B_2 can be excited through the excitation propagation with four possible channels: (i) $A_1 \to B_1, A_2 \to B_2$; (ii) $A_1 \to B_1, A_1 \to B_2$; (iii) $A_2 \to B_1, A_2 \to B_2$; (iv) $A_1 \to B_2, A_2 \to B_1$. All these propagations should be long enough so that nodes B_1 and B_2 can reexcite nodes A_1 and A_2, respectively. For a successful two-center excitation, each center should be effective, we thus require

$$L_{\min}(A_1,B_1), L_{\min}(A_2,B_2) \geq L_c. \tag{4a}$$

In order to make the above (iv) channel work, we require one more condition

$$L_{\min}(B_1 \to A_1 \to B_2 \to A_2) \geq 2L_c. \tag{4b}$$

Under conditions (4a) and (4b), the $(A_1,B_1)(A_2,B_2)$ excitation can cause a two-center target wave oscillation labeled as the $(A_1,B_1 \mid A_2,B_2)$ attractor. This two-center excitation fails whenever any of conditions (4a) and (4b) is violated.

Generally, we can make an n-center excitation (A_i,B_i) $i = 1,2,\ldots,n$, and the necessary and sufficiently conditions for the existence of the n-center target wave attractor are

$$\begin{aligned} &L_{\min}(A_{j_1},B_{j_1};A_{j_2},B_{j_2};\ldots;A_{j_q},B_{j_q}) \geq qL_c, \\ &q = 1,2,\ldots,n, \end{aligned} \tag{5}$$

which should be satisfied for all permutations of q indexes $j_1, j_2, \ldots, j_q$ selected from the set $(1,2,\ldots,n)$, and for all $q \in [1,n]$. The $L_{\min}(A_{j_1}, B_{j_1}; A_{j_2}, B_{j_2}; \ldots; A_{j_q}, B_{j_q})$ is defined as the shortest length linking all the given nodes with the given order. These conditions can be proven in the same spirit as conditions (2) and (4) that the excitation of any driver B_i can surely excite the corresponding center A_i after the refractory period of A_i. Whenever condition (5) is satisfied, the resulting oscillatory attractor is labeled as $(A_1,B_1 \mid A_2,B_2 \mid \cdots \mid A_n,B_n)$. Consider a sparse network ($\langle k \rangle \ll \ln N$) and a small center number ($n \ll N$), and assume a homogeneous random network with identical interaction degree $k_1 = k_2 = \cdots = k_N = k$, the number of n-center attractors can be estimated as

$$M_n \propto \frac{N(N-2)\cdots(N-2(n-1))}{n!}k^n = C_{N/2}^n (2k)^n, \tag{6}$$

which is an extremely large number for a large N and multiple centers.

Through the above analysis, we can now make a systematical investigation on various attractors with different labels. Considering the homogeneous random network in Fig. 5(a) with $N = 20$ and $k = 3$, we can easily predict and retrieve wanted oscillatory attractors. For instance, let us ask whether we can have an oscillatory attractor of label $(2,14)$ in the network, i.e., a target wave pattern with node 2 as the target center

and node 14 as its driver. We check the shortest loop passing both nodes 2 and 14 (the red loop in Fig. 5(b)), identify its length $L_{\min}(2,18) = 6 > L_c = 5$, and conclude that the attractor of the given label does exist. Secondly, we can surely retrieve this target wave attractor in the complex network by exciting node 2 with a stimulating pulse while blocking the excitation of its neighbor 18 simultaneously. And then the self-sustained target wave pattern is generated. In the same way, we can conclude that an oscillatory attractor of label $(9,3 \mid 4,20)$ also exists since condition (4) for a two-center target pattern is fulfilled ($L_{\min}(9,3) = L_{\min}(4,20) = 6 > L_c$, $L_{\min}(4 \to 3 \to 9 \to 20 \to 4) = 10 = 2L_c$). We simultaneously excite nodes 9 and 4 and temporarily block nodes 20 and 3 at the same time, then we successfully produce the $(9,3 \mid 4,20)$ two-center target wave attractor. Similar analysis and operation predict the existence of a two-center attractor of label $(5,13 \mid 15,12)$ and easily retrieve it from the all-rest state as shown in Fig. 5(d). Moreover, the oscillations can be easily terminated by suppressing the excitations of the center nodes only (node 2 for attractor $(2,18)$; nodes 9 and 4 for attractor $(9,3 \mid 4,20)$, and nodes 5 and 15 for attractor $(5,13 \mid 15,12)$) as shown in Fig. 5(e). On the other hand, by reading the topological structure in Fig. 5(a), we can easily conclude that one-center excitation $(1,8)$, two-center excitation $(14,10)(20,3)$, and three-center excitation $(9,17)(11,7)(15,8)$ cannot generate the corresponding target wave attractors because $L_{\min}(1,8) = 4 < L_c$ (no attractor labeled $(1,8)$), $L_{\min}(10 \to 14 \to 3 \to 20 \to 10) = 7 = 2L_c$ (no attractor labeled $(14,10 \mid 20,2)$, and $L_{\min}(17 \to 9 \to 7 \to 11 \to 8 \to 15 \to 17) = 14 < 3L_c$ (no attractor labeled $(9,17 \mid 11,7 \mid 15,8)$). All results in Fig. 5 verify our understanding on the target wave patterns, including their existences, simple retrieving, and suppressing operations.

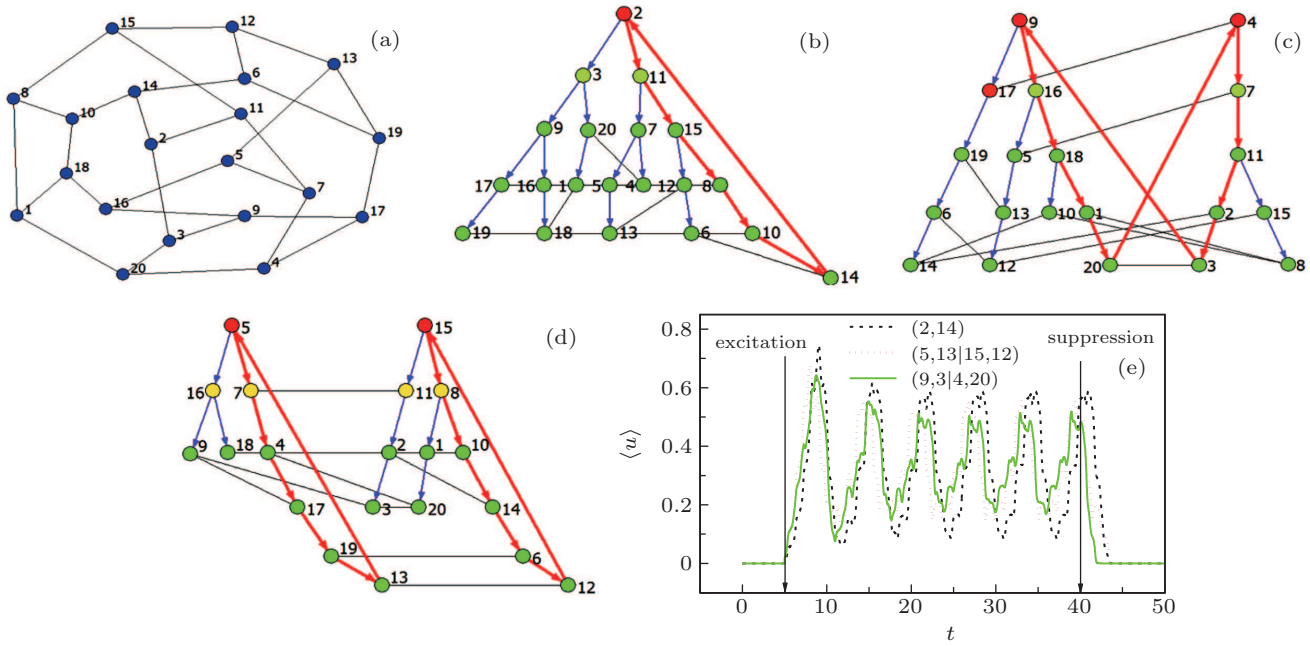


Fig. 5. Systematical topology analysis of a given network on labelable attractors. (a) Complex network considered with $N = 20$ and $k = 3$. (b) The 1-center attractor of label (2, 14) with $L_{\min}(2,14) = 6$. (c) and (d) The 2-center attractors of labels $(9,3|4,20)$ and $(5,13|15,12)$, satisfying all conditions of Eq. (4). In the former case, a longer loop passing through both pairs of key nodes serves as the oscillation source. In the latter case, two source loops (the red arrows) maintain the network oscillation. (e) Evolutions of $\langle u(t) \rangle$ by applying (2, 14) (black-dashed curve), $(9,3|4,20)$ (green solid curve), and $(5,13|15,12)$ (red dotted curve) excitations at $t = 5$. Oscillations in panels (b)–(d) are terminated by suppressing center 2, centers 9 and 4 simultaneously, and centers 5 and 15 simultaneously, respectively, at $t = 40$.[14]

5. Statistics on target wave patterns in ECNs

In Fig. 5, we show a few examples of target wave patterns with certain labels. In this section, we will systematically study the statistics of attractors on ECNs. First, we investigate the network in Fig. 5(a). In Fig. 6(a), we show the number of diverse periodic attractors found, M, against the number of tests, $\hat{T}$, from random initial conditions. Even for a very small network ($N = 20$), the number of attractors can easily exceed 10^3 (note that the slope in Fig. 6(a) is still not saturated to zero after 4.32 millions of tests despite about 10^3 attractors already explored). In Fig. 6(b), the number of different center attractors against $\hat{T}$ is plotted. We find that the 1-center attractor saturates to $M_1 = 42$ at a very small $\hat{T}$ ($\hat{T} < 10^3$), while 2-center M_2 and 3-center M_3 saturate successively for larger and larger $\hat{T}$'s ($M_2 = 245$ around $\hat{T} \approx 4 \times 10^5$, $M_3 = 145$ around $\hat{T} \approx 2 \times 10^6$). The numbers of M_1, M_2, and M_3 can be predicted by conditions (2), (4), and (5), respectively, and the predictions coincide exactly with the above numerical results. Another

interesting observation is that the probabilities for attractors of different centers to appear are substantially different, i.e., $P_{M_1} \approx 75.7\% \gg P_{M_2} \gg 19.8\% \gg P_{M_3} \approx 2.0\% \gg P_{M>M_3}$. The high probabilities of few-center attractors emphasize the importance of these simple target wave patterns. In Fig. 6(c), the frequencies of appearances of different attractors are shown (index q follows the rank of frequencies of different attractors). All the $M_1 = 44$ one-center attractors have the highest frequencies, and most of the $M_2 = 256$ two-center attractors have the next highest frequencies.

In Figs. 6(d)–6(f), we perform exactly the same analysis as that in Figs. 6(a)–6(c), respectively, with a network of $N = 100$ and $k = 3$. In Fig. 6(d), the increasing tendency of the M–$\hat{T}$ curve is far from saturation, indicating that a huge number of attractors are still not recovered after 9×10^5 different attractors has already been identified. The saturated $M_1 = 288$ and $M_2 = 37980$ in Fig. 6(e) verify perfectly the theoretical predictions based on conditions (2) and (4).

In the statistical computations in Fig. 6, we focus on two examples only. In Table 1, large scale theoretical calculations are listed based on Eqs. (2), (4), and (5) for different system sizes (from $N = 30$ to $N = 300$). All data in Table 1 are obtained by averaging 200 randomly constructed networks of $k = 3$. The numbers of 1-, 2-, 3-center target wave attractors are predicted from these networks. Several points about Table 1 should be emphasized. First, the number of labeled attractors increases very rapidly with both increasing system size N and increasing center number n. At $N = 100$, the number of 3-center attractors can reach the order of million, and this number can reach hundreds of millions for $N = 300$. Second, all these attractors are associated with the corresponding labels. From the labels, we can easily retrieve these attractors, suppress the existing oscillations of the attractors, and transfer from one attractor to another wanted one. Third, all attractors are theoretically predicted according to the network topology and conditions (2), (4), and (5). We have numerically generated 1-, 2-, 3-center attractors in Table 1 by randomly choosing 10^3 samples for each type, and compared the simulation results with the predictions in Table 1; the agreement is 100%.

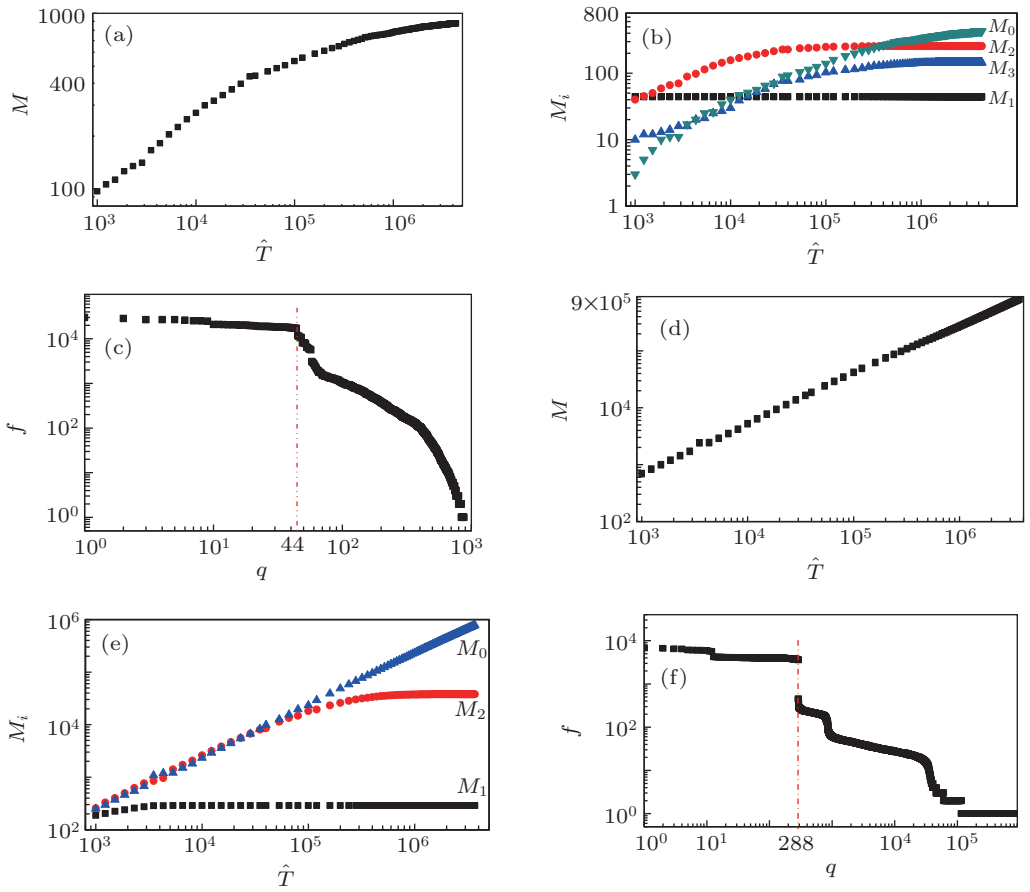


Fig. 6. Statistical results of labelable attractors obtained numerically. (a)–(c) Statistics on the network of Fig. 5(a). (a) The number of all numerically observed distinctive periodic attractors M versus the number of tests $\hat{T}$. Saturation is not reached after 4.32 million tests. (b) The M_i versus $\hat{T}$, M_1, M_2, and M_3 indicate the numbers of the centers, and M_0 is the number of all other periodic attractors. We observe saturation of M_1 to 44 firstly, and then saturations of M_2 and M_3 to 256 and 145 successively, which coincide perfectly with the results predicted by the topological analysis in Fig. 5(a). The M_0 has not reached saturation after 4.32 million tests. (c) Distribution of the appearance frequencies f of different attractors. The index of the attractor, q, is arranged according to the decreasing order of the appearance frequency f. All the largest 44 frequencies correspond to the 1-center attractors. (d)–(f) The same results as those in panels (a)–(c), respectively, for the network of Fig. 4(c) with $N = 100$ and $k = 3$. In panel (e), M_0 includes all periodic attractors other than M_1 and M_2. The numerically saturated $M_1 = 288$ and $M_2 = 37980$ agree perfectly with the predictions by the topology analysis.[14]

Table 1. Numbers of labels corresponding to the attractors of homogeneous ECNs with $k = 3$ and different system sizes N, and different numbers of centers n predicted by Eqs. (2), (4), and (5). All data for any given N are the averages of 200 different randomly constructed networks. Unlike Fig. 6 which shows statistics of distinctive attractors, here it is possible that several distinctive labels may correspond to the same attractor. The results of networks with high sparseness ($\ln N \gg k$) coincide with the predictions of Eqs. (2), (4), and (5).[14]

N	1-center	2-center	3-center
30	65	1202	8257
50	127	6279	147543
80	215	20607	1120672
100	276	34998	2646073
120	336	53017	5183945
150	427	87011	11431092
180	516	128733	20226353
200	575	160531	30452455
220	638	198536	42774730
250	726	257187	62099328
280	816	326384	88157634
300	877	378672	105239745

Now we come back to the memory function of the brain. The neural networks perform various functions of the brain. Memories in the brain are assumed by many biologists as attractors of dynamical neural networks.[30–33] The existence of many attractors, easy retrieves and suppressions of these attractors are necessary dynamic requests of the neural networks. In this paper, we find that ECNs do fulfill these requirements. ECNs can have huge numbers of attractors, and these attractors can be associated with individual labels. These labels clearly give clues to easy retrieves and suppressions of wanted and unwanted attractors. From the dynamic point of view, it is not difficult to image why neural networks, where the neurons have excitable dynamics and the interactions between the neurons have the structures of complex networks, can have the fascinating function of memories. Of course, actual memories in neural systems are certainly not the labelable target wave attractors of our ECNs. Moreover, how to construct memory attractors by learning, which is of crucial importance, has not been considered even slightly here. However, the study in this paper shows that simple dynamic systems can conduct seemly very complicated tasks by their collective activities in networks, and some elementary tasks required by the memory function can indeed be performed by complex networks consisting of excitable nodes.

6. Conclusion

In conclusion, we have studied the problem of oscillations of complex networks consisting of excitable nodes. A method of dominant phase advanced driving is proposed to explore the self-organized structures supporting the network oscillations, in particular, we investigate the oscillation sources and the main propagating paths in ECNs. A further study shows that many oscillatory patterns in ECNs are identified to the target waves in complex networks, which have center nodes generating target waves propagating throughout the networks and drivers of the centers keeping the centers to sustain the oscillations. And the shortest loops passing centers and the corresponding drivers are just the self-organized structure playing the role of sources of ECN oscillations. The target waves can be conveniently controlled (turned on or turned off) by controlling (stimulating or suppressing) the excitations of the centers.

Since for a target wave the center (say node A) and the driver (say node B) can uniquely determine the given target, (A,B) can serve as the label of this target wave attractor. Therefore, the dynamic problem of the target wave pattern formation can be treated as a topological problem of identification of different labels. Instead of numerically finding various target wave attractors, we just need to count various distinctive labels and study conditions (2), (4), and (5) for the existences of the target wave patterns with given labels. From the label study and the numerical verification, we find that the number of distinctive target wave attractors is huge for ECNs with large size N. And all these attractors can be easily retrieved or suppressed by manipulating a few key nodes (centers and drivers) according to the instructions of the labels. All the above features of the ECN attractors remind us the function of the memory of the brain. The multiplicity of the ECN attractors is similar to the rich memory attractors of the brain, while the labels of the attractors serve as the clues for searching and manipulating some given memories. Moreover, the excitability of local dynamics of nodes and the complexity of interaction network structures are two major features of the brain networks. It is however emphasized that labelable target wave patterns catch only some elementary dynamic features of the brain memory, and they are far from being the actual memory ingredients.

There are two possible directions for the future developments of the present work. One lies in the aspect of pattern formation and pattern dynamics of complex networks. In the present review, formation and dynamics of target wave patterns in ECNs have been studied in detail. Dynamics of other possible patterns together with their classification, features, and conditions also need to be investigated. Moreover, all the results in Sections 4 and 5 are based on an excitation propagation mechanism, called the logic excitation, i.e., any excited node can propagate excitations by successfully exciting all its neighbors in the rest state. This mechanism exists very commonly in ECNs for proper coupling strengths. However, in many cases, this logical excitation is not satisfied, and the extension of the present work to more general cases is an interesting and practical topic. The second direction is to apply the methods and results of the present work to realistic systems, in particular, to neural systems. In this regard, actual situations of neural networks, including electrical and chemical activi-

ties occurring in neurons and clusters of neurons, signal propagations in different brain areas, various brain functions like learning rules, inevitable existence of noise, and so on should be considered in the network dynamics. These make the problems incomparably complicated as well as much more interesting. They are our targets of long term research.

References

[1] Cross M C and Hohenberg P C 1993 *Rev. Mod. Phys.* **65** 851
[2] Meron E 1992 *Phys. Rep.* **218** 1
[3] Greenberg J M and Hastings S P 1978 *SIAM J. Appl. Math.* **34** 515
[4] Winfree A T 1987 *When Time Breaks Down* (Princeton: Princeton University Press)
[5] Tinsley M, Cui J, Chirila F V, Taylor A, Zhong S and Showalter K 2005 *Phys. Rev. Lett.* **95** 038306
[6] Müller-Linow M, Hilgetag C C and Hütt M T 2008 *PLos Comput. Biol.* **4** e1000190
[7] Watts D J and Strogatz S H 1998 *Nature* **393** 440
[8] Barabási A L and Albert R 1999 *Science* **286** 509
[9] Dorogovtsev S N and Goltsev A V 2008 *Rev. Mod. Phys.* **80** 1275
[10] Albert R and Barabási A L 2002 *Rev. Mod. Phys.* **74** 47
[11] Kuperman M and Abramson G 2001 *Phys. Rev. Lett.* **86** 2909
[12] Ji P, Peron T K D M, Menck P J, Rodrigues F A and Kurths J 2013 *Phys. Rev. Lett.* **110** 218701
[13] Liao X, Xia Q, Qian Y, Zhang L, Hu G and Mi Y 2011 *Phys. Rev. E* **83** 056204
[14] Mi Y, Zhang L, Huang X, Qian Y, Hu G and Liao X 2011 *Europhys. Lett.* **95** 58001
[15] Zhang Z, Ye W, Qian Y, Zheng Z, Huang X and Hu G 2012 *PLoS One* **7** e39355
[16] Mi Y, Liao X, Huang X, Zhang L, Gu W, Hu G and Wu S 2013 *Proc. Natl. Acad. Sci. USA* **110** E4931
[17] Belik V, Geisel T and Brockmann D 2011 *Phys. Rev. X* **1** 011001
[18] Liao X H, Qian Y, Mi Y Y, Huang X D, Xia Q Z and Hu G 2011 *Front. Phys.* **6** 124
[19] Liao X H, Ye W M, Huang X D, Xia Q Z, Huang X Q, Li P F, Qian Y, Huang X D and Hu G 2009 arXiv:0906.2356v3
[20] Fu C, Zhang H, Zhan M and Wang X 2012 *Phys. Rev. E* **85** 066208
[21] Zhang L, Gu W, Liao X, Wang Y, Hu G and Mi Y 2012 *Europhys. Lett.* **99** 18005
[22] Qian Y, Liao X, Huang X, Mi Y, Zhang L and Hu G 2010 *Phys. Rev. E* **82** 026107
[23] Bär M and Eiswirth M 1993 *Phys. Rev. E* **48** R1635
[24] D'Souza R M 2009 *Nat. Phys.* **5** 627
[25] Erdős P and Réyi A 1959 *Publ. Math. (Debrecen)* **6** 290
[26] Bollobás B 1998 *Modern Graph Theory* (New York: Springer-Verlag)
[27] Gerstner W and Kistler W M 2002 *Spiking Neuron Models* (Cambridge: Cambridge University Press)
[28] Moody S L, Wise S P, Pellegrino G di and Zipser D 1998 *J Neurosci* **18** 399
[29] Neiman T and Loewenstein Y 2013 *J Neurosci* **33** 1521
[30] Rabinovich M, Huerta R and Laurent G 2008 *Science* **321** 48
[31] Wills T J, Lever C, Cacucci F and Burgess N 2005 *Science* **308** 873
[32] Mazor O and Laurent G 2005 *Neuron* **48** 661
[33] Poucet B and Save E 2005 *Science* **308** 799